

Enhanced Pinning For Vortices in Hyperuniform Substrates and Emergent Hyperuniform Vortex States

Q. Le Thien^{1,2}, D. McDermott^{1,2}, C.J. Olson Reichhardt¹, and C. Reichhardt¹

¹ *Theoretical Division and Center for Nonlinear Studies,*

Los Alamos National Laboratory, Los Alamos, New Mexico 87545, USA

² *Department of Physics, Wabash College, Crawfordsville, Indiana 47933, USA*

(Dated: February 2, 2022)

Disordered hyperuniformity is a state of matter which has isotropic liquid like properties while simultaneously having crystalline like properties such as little variation in the density fluctuations over long distances. Such states arise for the packing of photoreceptor cells in chicken eyes, jammed particle assemblies, and in nonequilibrium systems. An open question is what possible applications could utilize properties of hyperuniformity. One of the major issues for applications of type-II superconductors is how to achieve high critical currents by preventing the motion or depinning of vortices, so there is great interest in understanding which pinning site geometries will lead to the optimal pinning of vortices. Here, using large scale computational simulations, we show that vortices in a type-II superconductor with a hyperuniform pinning arrangement exhibit enhanced pinning compared to an equal number of pinning sites with a purely random arrangement, and that the enhancement is robust over a wide range of parameters. The stronger pinning arises in the hyperuniform arrays due to the suppression of pinning density fluctuations, permitting higher pin occupancy and the reduction of weak links that lead to easy flow channeling. We also show that in general, in amorphous vortex states in the presence of either random or hyperuniform pinning arrays, the vortices themselves exhibit disordered hyperuniformity due to the repulsive nature of the vortex-vortex interactions.

Introduction—

Disordered hyperuniformity describes amorphous systems which have both liquid and crystalline properties [1, 2]. The amorphous nature of these systems means that they are isotropic, as opposed to crystalline systems which break spatial symmetries and exhibit Bragg peaks. Hyperuniform systems also show strong suppression of density fluctuations out to long length scales, a crystal-like property, where the density per unit cell is fixed at a constant value. This is in contrast to a random assembly or Poisson distribution of particles that can have large density variations since it is possible for points to accumulate in certain regions or to have extended regions devoid of points. In 2003, Torquato and Stillinger proposed that there are disordered many body systems in which density fluctuations are suppressed out to very long wave lengths, and that such systems can be characterized as exhibiting disordered hyperuniformity [1]. Since then, hyperuniformity has been studied in a growing number of systems including the ordering of photoreceptor cells in chicken eyes [3], jammed particle assemblies [4–6], block-copolymer systems [7], near nonequilibrium critical points [8–10], and even in certain quantum systems [11]. An open question is what possible applications there are for systems that exhibit disordered hyperuniformity. There have already been some proposals along these lines, such as the use of hyperuniformity to create photonic materials with complete band gaps [12].

Here, we show that pinning sites geometrically arranged to exhibit hyperuniformity have superior pinning properties compared to an equivalent number of randomly arranged pinning sites for magnetic vortices in a

type-II superconductor over a wide range of magnetic fields, substrate strengths, and applied drives. One of the major issues for applications of type-II superconductors is that the onset of vortex motion limits the value of the current that can be carried by the sample in the superconducting state, since the vortex motion produces dissipation through a voltage response [13–15]. There have been intense efforts directed at understanding ways to increase the pinning of vortices by adding defects to superconducting samples in order to locally suppress the superconducting order parameter, creating low energy regions that trap vortices [15, 16]. To emphasize the importance of pinning, a general rule of thumb is that doubling the critical current reduces the cost of using these materials by half [15]. Since adding defects to the sample can degrade the material response, there is a limit to the number of pinning sites that can be added. Therefore it is important to determine the best way to spatially distribute a fixed number of pinning sites to create the strongest pinning for a wide range of fields. One method is to arrange the pinning sites in crystalline lattices [17–23], diluted ordered lattices [24, 25], quasiperiodic arrangements [26, 27], conformal arrangements [28–30], or gradient arrays [31–33]. Typically in systems with crystalline arrangements of pinning sites, the depinning threshold is strongly enhanced over that of random pinning arrangements only for matching conditions under which the number of vortices is an integer multiple of the number of pinning sites, whereas under non-matching conditions, the periodic pinning arrays have lower depinning thresholds than random arrays since the high symmetry of the array allows easy 1D vortex flow channels

to form along symmetry directions of the crystal [20, 28]. In order to achieve strong pinning for a wide range of parameters, it would be ideal to place the pinning sites in a geometry that has reduced pinning density fluctuations, similar to crystalline arrays, while simultaneously remaining isotropic in order to eliminate easy flow symmetry channeling effects. This suggests that pinning geometries with disordered hyperuniformity could have ideal properties for vortex pinning.

Another question is whether amorphous assemblies of vortices in the presence of random pinning arrange themselves in a hyperuniform state or a random state. Generally, vortex structures in the presence of pinning are described as either being ordered, as in a Bragg glass state where there are no dislocations in the vortex lattice [34], or as amorphous where numerous topological defects are present [34–36]. Due to the repulsive interaction between vortices, strong density fluctuations are highly energetically costly, which suggests that the amorphous vortex structure may be hyperuniform in nature when vortex-vortex interactions are relevant, and more random in nature when pinning or thermal effects dominate. Since hyperuniform states are expected to occur for certain charged systems [2], pinned amorphous vortex systems may be ideal places to seek emergent hyperuniformity. We show that disordered hyperuniform vortex states arise for vortices interacting with either hyperuniform or random pinning arrays, which suggests that hyperuniformity is a general feature of pinned vortex systems. There are many techniques that have been used to visualize large amorphous vortex assemblies [37–45], and it would be interesting to re-examine this data to see if hyperuniform or random configurations occur. Additionally, there are a wide class of systems that have many similarities to amorphous vortices in the presence of pinning which may also exhibit hyperuniformity, including charge-stabilized colloids [46], Wigner crystals [47], and skyrmions in chiral magnets [48, 49].

System description—The key feature of disordered hyperuniformity is the suppression of density fluctuations out to long distances. This can be characterized in reciprocal space by the behavior of the structure factor $S(\mathbf{k}) = N_v^{-1} |\sum_i^{N_v} \exp(-i\mathbf{k} \cdot \mathbf{R}_i)|^2$, which goes to zero as $|\mathbf{k}|$ goes to zero, similar to a crystal; however, unlike a crystal, the hyperuniform $S(\mathbf{k})$ is isotropic and has no Bragg peaks [1, 2]. In general, for a disordered hyperuniform system $S(\mathbf{k})$ goes to zero as $|\mathbf{k}|^\alpha$, where α is a positive number. For a random system, $S(\mathbf{k})$ is isotropic but it approaches a finite value as $|\mathbf{k}|$ goes to zero.

We consider two-dimensional systems in which we place N_p pinning sites arranged in either a random or a hyperuniform configuration as shown in Fig. 1(a,b). The pinning sites are modeled as nonoverlapping local attractive parabolic wells with radius r_p . The hyperuniform array is constructed by setting up a square lattice of cells and placing one pinning site at a randomly chosen

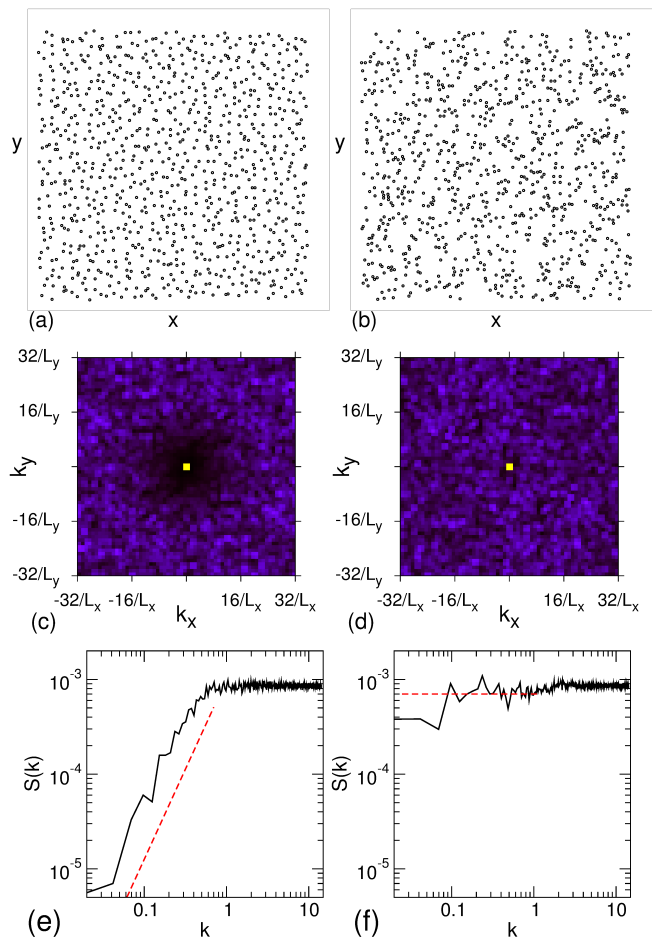


FIG. 1: The pinning site locations (open circles) for (a) a hyperuniform distribution and (b) a random distribution. (c) The corresponding structure factor $S(\mathbf{k})$ for the hyperuniform pinning array showing that the weight vanishes at small \mathbf{k} and that the system is isotropic. (d) $S(\mathbf{k})$ for the random pinning array, where the system is isotropic but the weight goes to a finite value at small \mathbf{k} . (e) $S(k)$ vs k for the hyperuniform array, where the dashed line is a fit to $S(k) \propto k^{1.9}$. (f) $S(k)$ vs k for the random array showing that $S(k)$ goes to a constant value at small k .

location within each cell [1, 2, 50]. The random array is constructed using a Poisson distribution. Figure 1(c,d) shows the corresponding $S(\mathbf{k})$ plots for the pinning configurations in Fig. 1(a,b). For the random array, $S(\mathbf{k})$ has constant weight at small \mathbf{k} , while for the hyperuniform array, the weight vanishes at small \mathbf{k} . In both cases $S(\mathbf{k})$ is isotropic, indicative of an amorphous system. In Fig. 1(e,f) we plot $S(k)$ versus k for the hyperuniform and random arrays, showing that $S(k)$ goes to zero at small k for the hyperuniform system, with the dashed line indicating a fit to $k^{1.9}$, while for the random array $S(k)$ goes to a constant value at small k . Within the sample we place N_v vortices modeled as point particles with a repulsion given by a pairwise Bessel function $K_1(r)$ interaction as used in previous vortex simulations

[20, 24, 28, 32]. The initial vortex positions are obtained by starting from a high temperature state and cooling to $T = 0$ to obtain a ground state configuration. After the initialization we apply a driving force, which experimentally corresponds to the application of an external current that creates a Lorentz force on the vortices. We wait a fixed time at each drive increment to ensure that the system has reached a steady state, and then we measure the average vortex velocity $\langle V \rangle = N_v^{-1} \sum_{i=1}^{N_v} \mathbf{v}_i \cdot \hat{\mathbf{x}}$ in the direction of the driving force to determine when the vortices depin and to construct velocity-force curves that are proportional to experimentally measurable current-voltage curves.

Numerical Methods— We utilize a particle model based on the London equations to describe the superconducting vortices. The dynamics of a single vortex i is governed by the following overdamped equation of motion:

$$\eta \frac{d\mathbf{R}_i}{dt} = \mathbf{F}_i^{vv} + \mathbf{F}_i^{vp} + \mathbf{F}^D, \quad (1)$$

where $\mathbf{v}_i = d\mathbf{R}_i/dt$ is the vortex velocity, \mathbf{R}_i is the vortex position, and η is the damping term which is set to unity. The interaction with the other vortices is repulsive and comes from the term $\mathbf{F}_i^{vv} = \sum_{j=1}^{N_v} F_0 K_1(R_{ij}/\lambda) \hat{\mathbf{r}}_{ij}$ where $F_0 = \phi_0^2/2\pi\mu_0\lambda^3$, ϕ_0 is the elementary flux quantum, μ_0 is the permittivity, $R_{ij} = |\mathbf{r}_i - \mathbf{r}_j|$, $\hat{\mathbf{r}}_{ij} = (\mathbf{r}_i - \mathbf{r}_j)/R_{ij}$, K_1 is the modified Bessel function which falls off exponentially for large R_{ij} , and λ is the London penetration depth which we set equal to 1.0. We place a cutoff on the interactions for vortex separations $R_{ij}/\lambda > 6.0$ for computational efficiency. At $T = 0$ and in the absence of pinning, the vortices form a triangular solid due to their mutually repulsive interactions. The pinning force \mathbf{F}_i^{vp} is produced by N_p non-overlapping harmonic potential traps with a radius $R_p = 0.15$ which can exert a maximum pinning force of F_p on a vortex. The driving term $\mathbf{F}^D = F_D \hat{\mathbf{x}}$ represents a Lorentz force from an externally applied current interacting with the magnetic flux carried by the vortices [26]. Our system is of size $L \times L$ with $L = 36$, and has periodic boundary conditions in the x and y directions. The vortex density is $n_v = N_v/L^2$ and the pinning density is $n_p = N_p/L^2$. In this work all forces are measured in units of F_0 and length in units of λ .

Enhanced Pinning with Hyperuniform Substrates—

In Fig. 2 we plot the the vortex velocity $\langle V \rangle$ vs applied driving force F_D for a system with $N_p = 900$ pinning sites at a pinning density of $n_p = 0.7$ with $F_p = 2.55$ arranged in either a hyperuniform or a random array. The depinning threshold is defined to be the lowest value of F_D for which a persistent flow of vortices occurs so that $\langle V \rangle > 0$. Since the vortex density is proportional to the magnetic field, we can define a matching field B_ϕ to be the field at which there is exactly one vortex per pinning site. At $B/B_\phi = 0.3$ in Fig. 2(a), the depinning threshold for the hyperuniform array is $F_c^{\text{hyper}}/F_p = 0.936$, while that of the random array is $F_c^{\text{random}}/F_p = 0.832$.

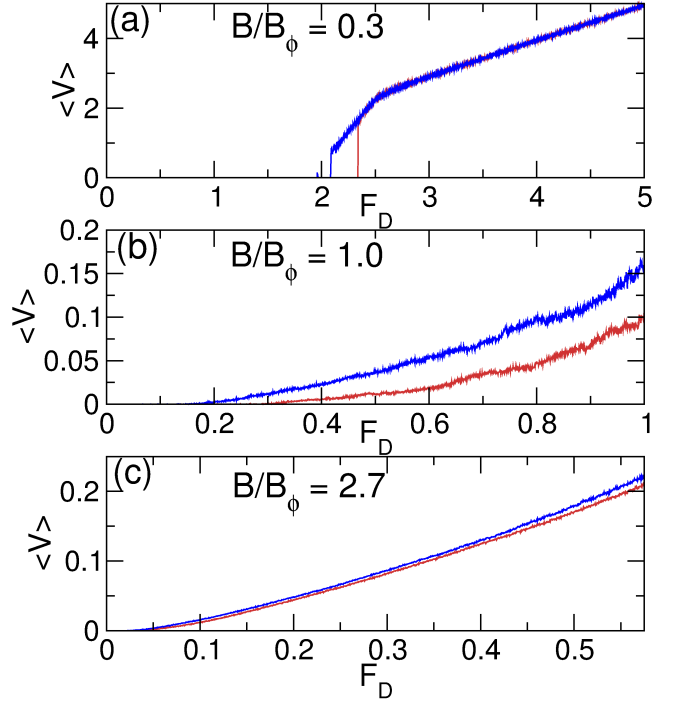


FIG. 2: Vortex velocity $\langle V \rangle$ vs driving force F_D for a hyperuniform pinning array (red, lower curves) and random pinning array (blue, upper curves) for systems with pinning density $n_p = 0.7$ and pinning strength $F_p = 2.55$. (a) $B/B_\phi = 0.3$, where B_ϕ is the field at which there is one vortex per pinning site. The ratio of the depinning threshold for the hyperuniform array to that of the random array is $R = 1.125$. (b) At $B/B_\phi = 1.0$, $R = 1.8$. (c) At $B/B_\phi = 2.7$, $R = 1.2$.

We quantify the pinning enhancement R as the ratio of these two depinning thresholds, $R = F_c^{\text{hyper}}/F_c^{\text{random}}$, obtaining $R = 1.125$ in this case. For $F_D/F_c^{\text{hyper}} > 1.0$, the velocity response for both pinning arrays is almost the same. In general, at lower fields where the vortices are widely spaced, the vortex-vortex interactions are less relevant and the depinning threshold is dominated by the strength of the individual pinning sites, so in the extremely low field limit of a single vortex, $R = 1.0$. At $B/B_\phi = 1.0$, Fig. 2(b) shows that the depinning threshold is more strongly enhanced by the hyperuniform array and $R = 1.8$. Here, once both systems have depinned, the velocity response for the random array is higher than that of the hyperuniform array, indicating that even within the sliding state, the hyperuniform array is more effective in reducing the dissipation. For $B/B_\phi = 2.7$ in Fig. 2(c), there is a reduced enhancement of $R = 1.2$, and above depinning, the velocity response of the hyperuniform array is slightly lower than that of the random array. In general, at the higher vortex densities, the vortex-vortex interactions begin to dominate over the vortex-pin interactions, so the difference in the pinning effectiveness of the two pinning geometries is reduced.

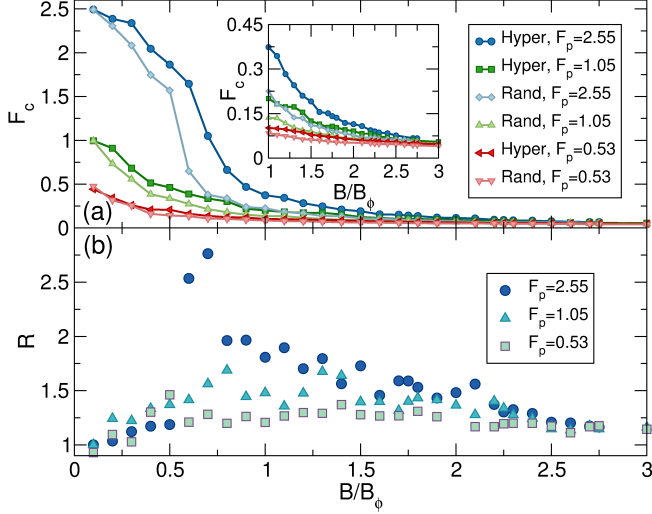


FIG. 3: (a) The depinning force F_c vs B/B_ϕ for hyperuniform arrays with $F_p = 2.55$ (dark blue circles), 1.05 (dark green squares), and 0.53 (dark red left triangles), and for random pinning arrays with $F_p = 2.55$ (light blue diamonds), 1.05 (light green up triangles), and 0.53 (orange down triangles). The inset shows a blow-up of the behavior at higher fields. (b) The depinning threshold ratio $R = F_c^{\text{hyper}}/F_c^{\text{random}}$ vs B/B_ϕ for $F_p = 2.55$ (dark blue circles), 1.05 (light blue triangles), and 0.53 (green squares), showing that the pinning is consistently enhanced for the hyperuniform pinning arrays.

In Fig. 3(a) we plot F_c^{hyper} and F_c^{random} versus B/B_ϕ for the system in Fig. 2 at varied pinning strengths of $F_p = 2.55, 1.05$, and 0.53 . For all cases, F_c decreases monotonically with increasing B/B_ϕ , and the hyperuniform arrays consistently have a higher F_c than the random arrays for a given value of F_p . Figure 3(b) shows the corresponding depinning threshold ratio R versus B/B_ϕ , where R approaches $R = 1.0$ in the $B/B_\phi = 0$ limit. In all cases there is an enhancement of F_c for the hyperuniform arrays, and the largest enhancement occurs over the range $0.5 < B/B_\phi < 2.5$. In this regime, the $F_p = 2.55$ system has some fields at which the enhancement is as large as $R = 2.75$. At higher values of B/B_ϕ , the vortex-vortex interactions begin to dominate over the pinning interactions, and the differences between the hyperuniform and random arrays are reduced.

In Fig. 4 we plot F_c^{hyper} and F_c^{random} versus pinning strength F_p at $B/B_\phi = 0.6$ and $B/B_\phi = 1.9$, while the inset shows the corresponding R vs F_p curves. The value of R can be as large as $R = 2.75$ for $B/B_\phi = 0.6$, but R falls to $R = 1.25$ for higher F_p when the pinning begins to dominate the behavior. For $B/B_\phi = 1.9$, the maximum enhancement is only $R = 1.5$, but the enhancement remains more robust out to higher values of F_p .

To better understand how the hyperuniform arrays produce enhanced pinning, in Fig. 5(a) we plot the fraction P_v of vortices located at pinning sites versus B/B_ϕ at $F_p = 2.55, 1.05$, and 0.53 for the random and hy-

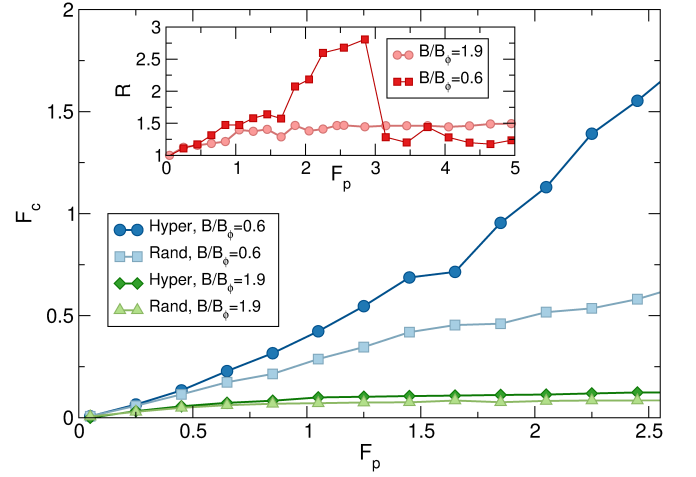


FIG. 4: The depinning force F_c vs F_p for hyperuniform arrays at $B/B_\phi = 0.6$ (dark blue circles) and $B/B_\phi = 1.9$ (dark green diamonds) and for random arrays at $B/B_\phi = 0.6$ (light blue squares) and $B/B_\phi = 1.9$ (light green triangles). Inset: the depinning current ratio R vs F_p for $B/B_\phi = 0.6$ (red squares) and $B/B_\phi = 1.9$ (pink circles).

peruniform arrays, showing that for any fixed value of F_p , a higher fraction of vortices are located at pinning sites for the hyperuniform array than for the random array. In Fig. 5(b) we plot P_v versus F_p for samples with $B/B_\phi = 1.9$ and 0.6 , where a similar trend appears. Figure 5(c,d) illustrates the vortex and pinning site locations in a small section of the sample for $B/B_\phi = 1.9$ and $F_p = 2.55$. Here, there are five unoccupied pinning sites in the hyperuniform array in Fig. 5(c), while there are eleven unoccupied pinning sites in the random array in Fig. 5(d). In the random array, local clumping of the pinning site positions can occur, and if a vortex is trapped by one pinning site in such a clump, its repulsive force can screen the remaining pins and prevent other vortices from occupying them. The random array can also contain large spatial regions in which there are no pinning sites, and vortices located in these regions can flow relatively easily along river-like channels or weak links, depressing the value of F_c . In the hyperuniform array, pinning density fluctuations are suppressed, so there is less screening of the pinning sites and a correspondingly higher pin occupation fraction, as shown in Fig. 5. In periodic pinning arrays, pinning density fluctuations are absent; however, due to the symmetry of the pinning lattice, there are easy flow directions along which vortices can form one-dimensional easy-flow channels, particularly at incommensurate fillings [32]. It may be possible to construct other types of hyperuniform arrays beyond the ones we consider here which would allow for even stronger enhancement of the pinning, or to create a pinning lattice that is hyperuniform along only one direction.

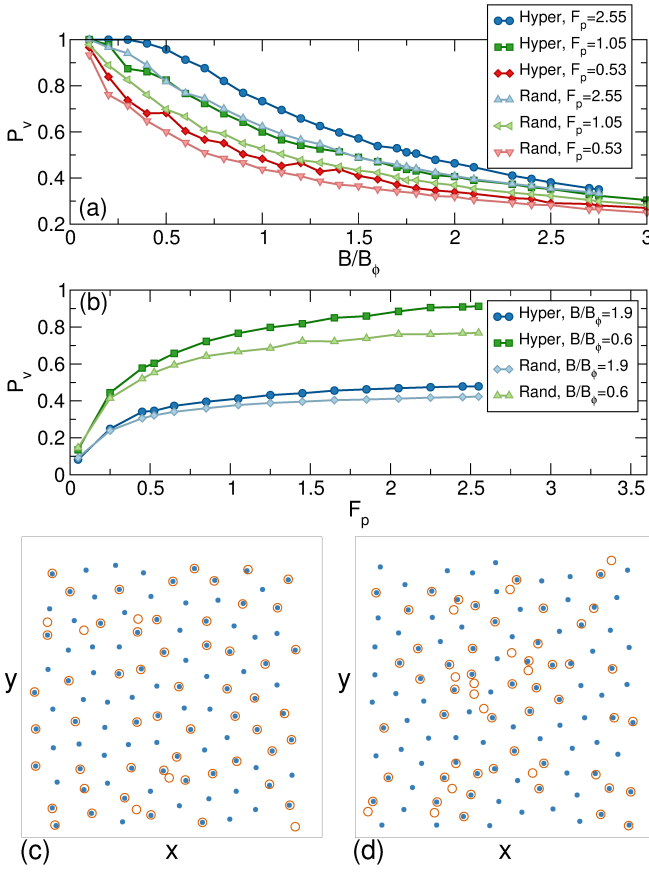


FIG. 5: (a) Fraction P_v of vortices located at pinning sites vs B/B_ϕ for hyperuniform arrays at $F_p = 2.55$ (dark blue circles), 1.05 (dark green squares), and 0.53 (red diamonds), and random arrays at $F_p = 2.55$ (light blue up triangles), 1.05 (light green left triangles), and 0.53 (orange down triangles), showing that there is a consistently higher fraction of occupied pinning sites in the hyperuniform arrays. (b) P_v vs F_p for hyperuniform arrays at $B/B_\phi = 1.9$ (dark blue circles) and 0.6 (dark green squares) and random arrays at $B/B_\phi = 1.9$ (light blue diamonds) and 0.6 (light green triangles), showing a similar trend. (c) The vortex (blue filled circles) and pinning site (orange open circles) locations in a small portion of the sample for a hyperuniform array at $F_p = 2.55$ and $B/B_\phi = 1.5$. (d) Vortex (blue filled circles) and pinning site (orange open circles) locations in a small portion of the sample for the random array under the same conditions showing that a higher fraction of pinning sites are unoccupied.

Emergent Hyperuniformity in Vortex Systems

We next consider whether amorphous vortex configurations in the presence of random or hyperuniform pinning arrays exhibit hyperuniformity. As described above, disordered hyperuniform systems have two identifying characteristics in the structure factor: $S(\mathbf{k})$ is isotropic, and it goes to zero at small $|\mathbf{k}|$. In Fig. 6(a,b,c) we show $S(k)$ of the vortex configuration for a random pinning array at $n_p = 0.7$ with $F_p = 0.55$, 1.05, and 2.55 for $B/B_\phi = 0.6$, 1.9, and 2.7, while in Fig. 6(d,e,f) we plot the same quantities for vortices interacting with a hyper-

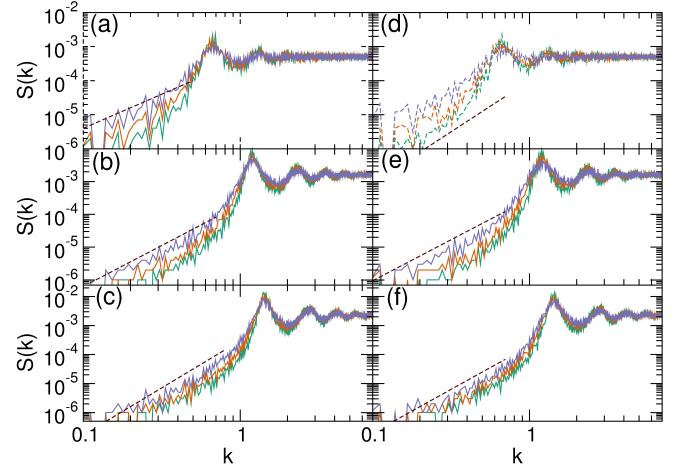


FIG. 6: (a,b,c) $S(k)$ of the vortex positions vs k for $n_p = 0.7$ at $F_p = 0.55$ (green), 1.05 (orange), and 2.55 (purple) for a random pinning array at (a) $B/B_\phi = 0.6$, (b) $B/B_\phi = 1.9$, and (c) $B/B_\phi = 2.7$. In each case k goes to zero as a power law, as indicated by the dashed line which is a power law fit with exponent (a) $\alpha = 2.0$, (b) $\alpha = 2.5$, and (c) $\alpha = 3.25$. (d,e,f) $S(k)$ of the vortex positions vs k for $n_p = 0.7$ at the same F_p values as above for a hyperuniform pinning array at (d) $B/B_\phi = 0.6$, (e) $B/B_\phi = 1.9$, and (f) $B/B_\phi = 2.7$. Dashed lines indicate power law fits with exponents of (d) $\alpha = 3.0$, (e) $\alpha = 2.5$, and (f) $\alpha = 3.0$.

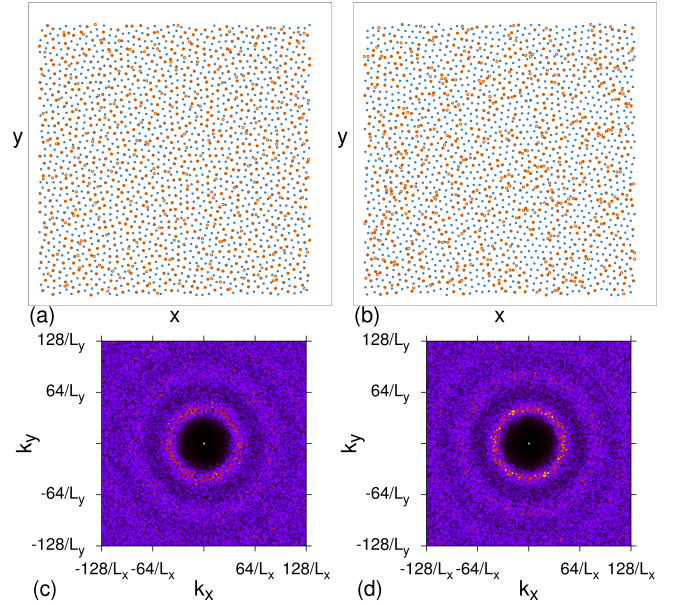


FIG. 7: Vortex (blue filled circles) and pinning site (orange open circles) location in the entire sample at $B/B_\phi = 1.9$ at $F_p = 2.55$ for (a) a hyperuniform pinning array and (b) a random pinning array. (c) Structure factor $S(\mathbf{k})$ for the vortex positions in panel (a). (d) $S(\mathbf{k})$ for the vortex positions in panel (b).

runiform pinning array. In each case the vortices form an amorphous structure, as shown in Fig. 7(a,b) for the hyperuniform and random arrays at $B/B_\phi = 1.9$ and $F_p = 2.55$. The corresponding plots of $S(\mathbf{k})$ for the *vortex* configurations appear in Fig. 7(c,d), and show a ring feature in each case indicating that the vortices are arranged isotropically. In Fig. 6, all of the curves in all of the panels exhibit a power law decay, with $S(k)$ going to zero as $S(k) \propto k^\alpha$ with α in the range $\alpha = 2.5$ to $\alpha = 3.5$, as indicated by the dashed lines. In general, if F_p is large or the vortex-vortex interactions are weak, the vortex configurations are dominated by the configuration of the pinning sites, so in the random pinning array system the vortices would exhibit random characteristics, with $S(\mathbf{k})$ going to a constant value as $k \rightarrow 0$. In real superconductors, the vortex-vortex interaction strength is non-monotonic as a function of field and temperature, and it goes to zero as the upper critical field or critical temperature is approached. It is therefore possible that a transition could occur from a crystalline to a hyperuniform amorphous vortex state, followed by a second transition to a truly amorphous random or liquid vortex state as a function of increasing field or increasing temperature. There are already numerous experimental observations of amorphous vortex states with and without large density fluctuations at higher magnetic fields [42–45], and it would be interesting to reexamine this experimental data to determine whether the vortex configurations appear to be random or hyperuniform.

In Fig. 8(a) we show a proposed generic phase diagram for repulsively interacting particle systems as a function of temperature versus the strength of the quenched disorder F_p . At high temperatures or for strong disorder, the system is amorphous and the particle positions have random or liquid-like characteristics. Between the crystalline state and the random or liquid state we propose that a disordered hyperuniform state exists for intermediate disorder strength.

In Fig. 8(b) we illustrate a proposed variation of the vortex phase diagram for a high temperature superconductor [34–36] in the presence of quenched disorder. Due to the nonmonotonic behavior of the effective vortex-vortex interactions as function of magnetic field and temperature, there is a transition from a Bragg glass state at lower fields where the vortices are dislocation-free to an amorphous vortex glass state for increasing field or increasing temperature, while at high fields or temperatures, a vortex liquid phase appears. We conjecture that between the Bragg glass and the true random amorphous vortex glass, there is a state in which the vortex arrangement is amorphous but has hyperuniform properties. We note that for some systems, there can also be reentrant disordered phases at lower fields where the vortices are far apart and the pinning becomes dominant again, so this reentrant region could be another place to look for a crossover from hyperuniform to random disordered vor-

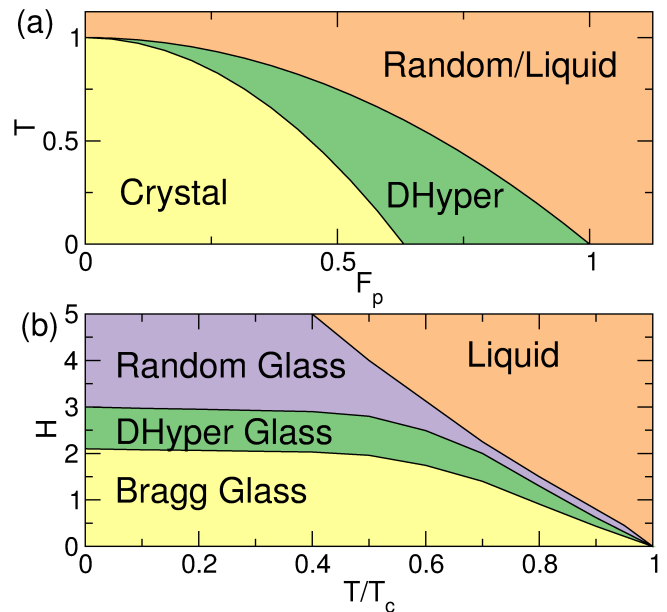


FIG. 8: (a) Schematic proposed phase diagram of temperature T vs disorder strength F_p for a system of repulsively interacting particles in the presence of quenched disorder. Between the crystalline and random or liquid state, there could be a disordered hyperuniform state (DHypcr). (b) Schematic proposed modified vortex phase diagram for a high temperature superconductor as a function of magnetic field H in arbitrary units vs reduced temperature T/T_c , where T_c is the critical temperature of the material. As a function of increasing H , there is a transition from a dislocation-free Bragg glass into a disordered hyperuniform state, followed by transitions to random amorphous or liquid states for high fields and temperatures.

tex arrangements. Data from imaging or neutron scattering experiments could show whether the vortex configurations are hyperuniform at the transition between the Bragg glass and an amorphous state, and whether at higher magnetic fields the vortices adopt a truly random configuration.

Discussion— We have shown that pinning sites in a disordered hyperuniform arrangement provide enhanced pinning compared to an equivalent number of randomly placed pinning sites. In hyperuniform arrays, the structure is isotropic like a liquid; however, the density fluctuations in the pinning site locations are strongly reduced out to large distances, similar to what is found in a crystal. Random arrays are also isotropic but can have strong density fluctuations of the type found in liquids. In the hyperuniform pinning arrays, we find that the probability for pinning site occupation is enhanced, while weak links or easy flow channels are minimized due to the isotropic nature of the pinning arrangement. There are no symmetry directions along which easy vortex flow can occur, unlike in crystalline pinning arrays. We also show that amorphous vortex states in the presence of random

or hyperuniform pinning arrays themselves exhibit hyperuniformity due to the repulsive nature of the vortex-vortex interactions, and we propose that there may be additional phases in the vortex phase diagram, including both hyperuniform and random amorphous phases. Our results should be general to the wider class of systems of repulsively interacting particles in the presence of either random or hyperuniform pinning arrays, including Wigner crystals, colloids, disordered charge systems, and skyrmions in chiral magnets.

We gratefully acknowledge the support of the U.S. Department of Energy through the LANL/LDRD program for this work. This work was carried out under the auspices of the NNSA of the U.S. DoE at LANL under Contract No. DE-AC52-06NA25396 and through the LANL/LDRD program.

-
- [1] Torquato, S. & Stillinger, F.H. Local density fluctuations, hyperuniformity, and order metrics. *Phys. Rev. E* **68**, 041113 (2003).
 - [2] Torquato, S. Hyperuniformity and its generalizations. *Phys. Rev. E* **94**, 022122 (2016).
 - [3] Jiao, Y., Lau, T., Hatzikirou, H., Meyer-Hermann, M., Corbo, J.C. & Torquato, S. Avian photoreceptor patterns represent a disordered hyperuniform solution to a multi-scale packing problem. *Phys. Rev. E* **89**, 022721 (2014).
 - [4] Zachary, C.E., Jiao, Y. & Torquato, S. Hyperuniform long-range correlations are a signature of disordered jammed hard-particle packings. *Phys. Rev. Lett.* **106**, 178001 (2011).
 - [5] Dreyfus, R., Xu, Y., Still, T., Hough, L.A., Yodh, A.G. & Torquato, S. Diagnosing hyperuniformity in two-dimensional, disordered, jammed packings of soft spheres. *Phys. Rev. E* **91**, 012302 (2015).
 - [6] Atkinson, S., Zhang, G., Hopkins, A.B. & Torquato, S. Critical slowing down and hyperuniformity on approach to jamming. *Phys. Rev. E* **94**, 012902 (2016).
 - [7] Zito, G., Rusciano, G., Pesce, G., Malafronte, A., Di Girolamo, R., Ausanio, G., Vecchione, A. & Sasso, A. Nanoscale engineering of two-dimensional disordered hyperuniform block-copolymer assemblies. *Phys. Rev. E* **92**, 050601 (2015).
 - [8] Hexner D. & Levine D. Hyperuniformity of critical absorbing states. *Phys. Rev. Lett.* **114**, 110602 (2015).
 - [9] Weijs, J.H., Jeanneret, R., Dreyfus, R. & Bartolo, D. Emergent hyperuniformity in periodically driven emulsions. *Phys. Rev. Lett.* **115**, 108301 (2015).
 - [10] Tjhung, E. & Berthier, L. Hyperuniform density fluctuations and diverging dynamic correlations in periodically driven colloidal suspensions, *Phys. Rev. Lett.* **114**, 148301 (2015).
 - [11] Torquato, S., Scardicchio, A. & Zachary, C.E. Point processes in arbitrary dimension from Fermionic gases, random matrix theory, and number theory. *J. Stat. Mech.: Theory Exp.* **2008**, P11019 (2008).
 - [12] Man, W., Florescu, M., Williamson, E.P., He, Y., Hashemizad, S.R., Leung, B.Y.C., Liner, D.R., Torquato, S., Chaikin, P.M. & Steinhardt, P.J. Isotropic band gaps and freeform waveguides observed in hyperuniform disordered photonic solids. *Proc. Natl. Acad. Sci. (USA)* **110**, 15886 (2013).
 - [13] Blatter, G., Feigelman, M.V., Geshkenbein, V.B., Larkin, A.I. & Vinokur, V.M. Vortices in high-temperature superconductors. *Rev. Mod. Phys.* **66**, 1125 (1994).
 - [14] Larbalestier, D., Gurevich, A., Feldmann, D.M. & Polyanskii, A. High- T_c superconducting materials for electric power applications. *Nature* **414**, 368–377 (2001).
 - [15] Foltyn, S.R., Civale, L., Macmanus-Driscoll, J.L., Jia, Q.X., Maiorov, B., Wang, H. & Maley, M. Materials science challenges for high-temperature superconducting wire. *Nature Mater.* **6**, 631–642 (2007).
 - [16] Maiorov, B., Baily, S.A., Zhou, H., Ugurlu, O., Kennison, J.A., Dowden, P.C., Holesinger, T.G., Foltyn, S.R. & Civale, L. Synergetic combination of different types of defect to optimize pinning landscape using BaZrO₃-doped YBa₂Cu₃O₇. *Nature Mater.* **8**, 398–404 (2009).
 - [17] Baert, M., Metlushko, V.V., Jonckheere, R., Moshchalkov, V.V. & Bruynseraede, Y. Composite flux-line lattices stabilized in superconducting films by a regular array of artificial defects. *Phys. Rev. Lett.* **74**, 3269 (1995).
 - [18] Harada, K., Kamimura, O., Kasai, H., Matsuda, T., Tonomura, A. & Moshchalkov, V.V. Direct observation of vortex dynamics in superconducting films with regular arrays of defects. *Science* **274**, 1167 (1996).
 - [19] Martín, J.I., Vélez, M., Nogués, J. & Schuller, I.K. Flux pinning in a superconductor by an array of submicrometer magnetic dots. *Phys. Rev. Lett.* **79**, 1929 (1997).
 - [20] Reichhardt, C., Olson, C.J. & Nori, F. Commensurate and incommensurate vortex states in superconductors with periodic pinning arrays. *Phys. Rev. B* **57**, 7937 (1998).
 - [21] Berdiyrov, G.R., Milosevic, M.V. & Peeters, F.M. Novel commensurability effects in superconducting films with antidot arrays. *Phys. Rev. Lett.* **96**, 207001 (2006).
 - [22] Swiecicki, I., Ulysse, C., Wolf, T., Bernard, R., Bergeal, N., Briatico, J., Faini, G., Lesueur, J. & Villegas, J.E. Strong field-matching effects in superconducting YBa₂Cu₃O_{7- δ} films with vortex energy landscapes engineered via masked ion irradiation. *Phys. Rev. B* **85**, 224502 (2012).
 - [23] Latimer, M.L., Berdiyrov, G.R., Xiao, Z.L., Peeters, F.M. & Kwok, W.K. Realization of artificial ice systems for magnetic vortices in a superconducting MoGe thin film with patterned nanostructures. *Phys. Rev. Lett.* **111**, 067001 (2013).
 - [24] Reichhardt C. & Reichhardt C.J.O. Commensurability effects at nonmatching fields for vortices in diluted periodic pinning arrays. *Phys. Rev. B* **76**, 094512 (2007).
 - [25] Kemmler, M., Bothner, D., Ilin, K., Siegel, M., Kleiner, R. & Koelle, D. Suppression of dissipation in Nb thin films with triangular antidot arrays by random removal of pinning sites. *Phys. Rev. B* **79**, 184509 (2009).
 - [26] Misko, V., Savel'ev, S. & Nori, F. Critical currents in quasiperiodic pinning arrays: Chains and Penrose lattices. *Phys. Rev. Lett.* **95**, 177007 (2005).
 - [27] Kemmler, M., Gürlich, C., Sterk, A., Pöhler, H., Neuhaus, M., Siegel, M., Kleiner, R. & Koelle, D. Commensurability effects in superconducting Nb films with quasiperiodic pinning arrays. *Phys. Rev. Lett.* **97**, 147003 (2006).
 - [28] Ray, D., Reichhardt, C.J.O., Jankó, B. & Reichhardt, C.

- Strongly enhanced pinning of magnetic vortices in type-II superconductors by conformal crystal arrays. *Phys. Rev. Lett.* **110**, 267001 (2013).
- [29] Wang, Y.L., Latimer, M.L., Xiao, Z.L., Divan, R., Ocola, L.E., Crabtree, G.W. & Kwok, W.K. Enhancing the critical current of a superconducting film in a wide range of magnetic fields with a conformal array of nanoscale holes. *Phys. Rev. B* **87**, 220501(R) (2013).
- [30] Guénon, S., Rosen, Y.J., Basaran, A.C. & Schuller, I.K. Highly effective superconducting vortex pinning in conformal crystals. *Appl. Phys. Lett.* **102**, 252602 (2013).
- [31] Motta, M., Colauto, F., Ortiz, W.A., Fritzsche, J., Cuppens, J., Gillijns, W., Moshchalkov, V.V., Johansen, T.H., Sanchez, A. & Silhanek, A.V. Enhanced pinning in superconducting thin films with graded pinning landscapes. *Appl. Phys. Lett.* **102**, 212601 (2013).
- [32] Ray, D., Reichhardt, C. & Reichhardt, C.J.O. Pinning, ordering, and dynamics of vortices in conformal crystal and gradient pinning arrays. *Phys. Rev. B* **90**, 094502 (2014).
- [33] Wang, Y.L., Thoutam, L.R., Xiao, Z.L., Shen, B., Pearson, J.E., Divan, R., Ocola, L.E., Crabtree, G.W. & Kwok, W.K. Enhancing superconducting critical current by randomness. *Phys. Rev. B* **93**, 045111 (2016).
- [34] Giamarchi T. & Le Doussal, P. Phase diagrams of flux lattices with disorder. *Phys. Rev. B* **55**, 6577 (1997).
- [35] Beidenkopf, H., Avraham, N., Myasoedov, Y., Shtrikman, H., Zeldov, E., Rosenstein, B., Brandt, E.H. & Tamegai T. Equilibrium first-order melting and second-order glass transitions of the vortex matter in $\text{Bi}_2\text{Sr}_2\text{CaCu}_2\text{O}_8$. *Phys. Rev. Lett.* **95**, 257004 (2005).
- [36] Kwok, W.-K., Welp, U., Glatz, A., Koshelev, A.E., Kihlstrom, K.J. & Crabtree, G.W. Vortices in high-performance high-temperature superconductors. *Rep. Prog. Phys.* **79**, 116501 (2016).
- [37] Moser A., Hug, H.J., Parashikov, I., Stiefel, B., Fritz, O., Thomas, H., Baratoff, A., Güntherodt, H.-J. & Chaudhari, P. Observation of single vortices condensed into a vortex-glass phase by magnetic force microscopy. *Phys. Rev. Lett.* **74**, 1847 (1995).
- [38] Goa, P.E., Hauglin, H., Baziljevich, M., Il'yashenko, E., Gammel, P.L. & Johansen, T.H. Real-time magneto-optical imaging of vortices in superconducting NbSe_2 . *Supercond. Sci. Technol.* **14**, 729 (2001).
- [39] Fasano, Y. & Menghini, M. Magnetic-decoration imaging of structural transitions induced in vortex matter. *Supercond. Sci. Technol.* **21**, 023001 (2008).
- [40] Petrović, A.P., Fasano, Y., Lortz, R., Senatore, C., Demuer, A., Antunes, A.B., Paré, A., Salloum, D., Gougeon, P., Potel, M. & Fischer, Ø. Real-space vortex glass imaging and the vortex phase diagram of SnMo_6S_8 . *Phys. Rev. Lett.* **103**, 257001 (2009).
- [41] Auslaender, O.M., Luan, L., Straver, E.W.J., Hoffman, J.E., Koshnick, N.C., Zeldov, E., Bonn, D.A., Liang, R., Hardy, W.N. & Moler, K.A. Mechanics of individual isolated vortices in a cuprate superconductor. *Nature Phys.* **5**, 35–39 (2009).
- [42] Song, C.-L., Yin, Y., Zech, M., Williams, T., Yee, M., Chen, G.-F., Luo, J.-L., Wang, N.-L., Hudson, E.W. & Hoffman, J.E. Dopant clustering, electronic inhomogeneity, and vortex pinning in iron-based superconductors. *Phys. Rev. B* **87**, 214519 (2013).
- [43] Guillamón, I., Córdoba, R., Sesé, J., De Teresa, J.M., Ibarra, M.R., Viera, S. & Suderow, H. Enhancement of long-range correlations in a 2D vortex lattice by an incommensurate 1D disorder potential. *Nature Phys.* **10**, 851 (2014).
- [44] Ganguli, S.C., Singh, H., Saraswat, G., Ganguly, R., Bagwe, V., Shirage, P., Thamizhavel, A. & Raychaudhuri, P. Disordering of the vortex lattice through successive destruction of positional and orientational order in a weakly pinned $\text{Co}_{0.0075}\text{NbSe}_2$ single crystal. *Sci. Rep.* **5**, 10613 (2015).
- [45] Kremen, A., Wissberg, S., Haham, N., Persky, E., Frenkel, Y. & Kalisky, B. Mechanical control of individual superconducting vortices. *Nano Lett.* **16**, 1626–1630 (2016).
- [46] Deutschländer, S., Horn, T., Löwen, H., Maret, G. & Keim, P. Two-dimensional melting under quenched disorder. *Phys. Rev. Lett.* **111**, 098301 (2013).
- [47] Cha, M.-C. & Fertig, H.A. Topological defects, orientational order, and depinning of the electron solid in a random potential. *Phys. Rev. B* **50**, 14368 (1994).
- [48] Yu, X., Kikkawa, A., Morikawa, D., Shibata, K., Tokunaga, Y., Taguchi, Y. & Tokura, Y. Variation of skyrmion forms and their stability in MnSi thin plates. *Phys. Rev. B* **91**, 054411 (2015).
- [49] Reichhardt, C., Ray, D. & Reichhardt, C.J.O. Collective transport properties of driven skyrmions with random disorder. *Phys. Rev. Lett.* **114**, 217202 (2015).
- [50] Gabrielli, A. & Torquato, S. Voronoi and void statistics for super-homogeneous point processes. *Phys. Rev. E* **70**, 041105 (2004).